molecular pharmaceutics

pubs.acs.org/molecularpharmaceutics

Article

Selective Delivery of Dicarboxylates to Mitochondria by Conjugation to a Lipophilic Cation via a Cleavable Linker

Hiran A. Prag,[#] Duvaraka Kula-Alwar,[#] Laura Pala, Stuart T. Caldwell, Timothy E. Beach, Andrew M. James, Kourosh Saeb-Parsy, Thomas Krieg, Richard C. Hartley,* and Michael P. Murphy*

Cite This: *Mol. Pharmaceutics* 2020, 17, 3526−3540

Read Online

ACCESS | Metrics & More | Article Recommendations | Supporting Information

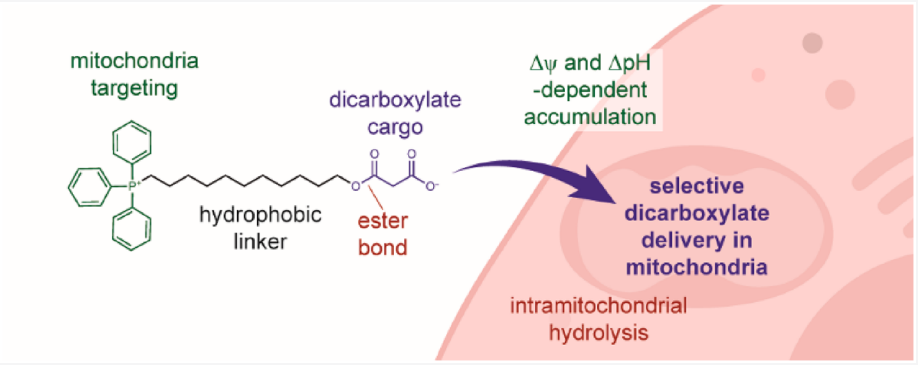

ABSTRACT: Many mitochondrial metabolites and bioactive molecules contain two carboxylic acid moieties that make them unable to cross biological membranes. Hence, there is considerable interest in facilitating the uptake of these molecules into cells and mitochondria to modify or report on their function. Conjugation to the triphenylphosphonium (TPP) lipophilic cation is widely used to deliver molecules selectively to mitochondria in response to the membrane potential. However, permanent attachment to the cation can disrupt the biological function of small dicarboxylates. Here, we have developed a strategy using TPP to release dicarboxylates selectively within mitochondria. For this, the dicarboxylate is attached to a TPP compound via a single ester bond, which is then cleaved by intramitochondrial esterase activity, releasing the dicarboxylate within the organelle. Leaving the second carboxylic acid free also means mitochondrial uptake is dependent on the pH gradient across the inner membrane. To assess this strategy, we synthesized a range of TPP monoesters of the model dicarboxylate, malonate. We then tested their mitochondrial accumulation and ability to deliver malonate to isolated mitochondria and to cells, *in vitro* and *in vivo*. A TPP−malonate monoester compound, TPP_{11}−malonate, in which the dicarboxylate group was attached to the TPP compound via a hydrophobic undecyl link, was most effective at releasing malonate within mitochondria in cells and *in vivo*. Therefore, we have developed a TPP−monoester platform that enables the selective release of bioactive dicarboxylates within mitochondria.

KEYWORDS: *mitochondria, lipophilic cation, mitochondriatargeting, dicarboxylate delivery, esterase*

INTRODUCTION

Mitochondria are essential for a wide range of cellular processes, and mitochondrial dysfunction plays a critical role in the pathology of numerous diseases.[1−3] Consequently, there is considerable interest in targeting molecules selectively to these organelles to report on and modify mitochondrial processes.[1,4] To do this, a molecule is often targeted using a delivery vector that selectively accumulates within mitochondria.[5−9] A common approach is by conjugation to the lipophilic triphenylphosphonium (TPP) cation, which is membrane permeable and drives the selective accumulation of attached moieties within mitochondria in cells and *in vivo*.[6,10,11] TPP cations achieve >100−1000-fold accumulation within mitochondria due to their uptake driven by the large mitochondrial membrane potential, as well as the potential across the plasma membrane.[6,10−12] This approach has been used extensively to target a range of probe and drug molecules to mitochondria *in vivo*, providing both new insights into mitochondrial biology and potential therapies.[8,13−18]

The inner mitochondrial membrane (IMM) presents a significant barrier to the delivery of charged molecules to mitochondria and possesses only a limited number of mitochondrial transporter proteins.[19] However, the large

Received: May 16, 2020
Revised: July 17, 2020
Accepted: July 21, 2020
Published: July 21, 2020

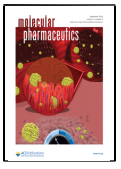

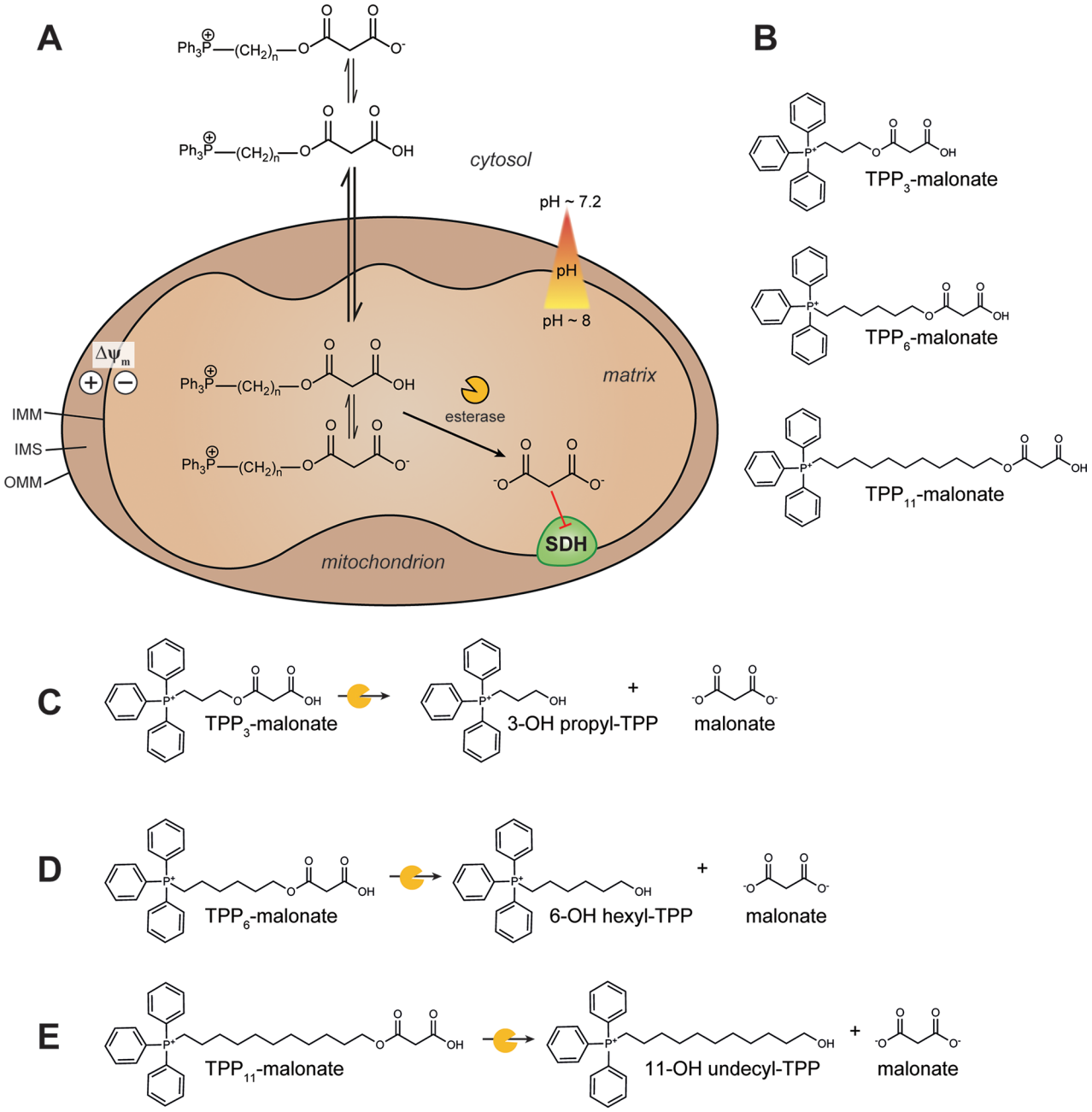

Figure 1. Mitochondria-targeted delivery strategy for the dicarboxylate malonate. (A) Theoretical uptake and hydrolysis of TPP−malonate monoesters in mitochondria. Abbreviations: OMM, outer mitochondrial membrane; IMM, inner mitochondrial membrane; IMS, intermembrane space; SDH, succinate dehydrogenase; $\Delta\psi_m$, mitochondrial membrane potential. (B−E) Structures of TPP−malonate monoesters synthesized (B) and hydrolysis schemes for TPP_3−malonate (C), TPP_6−malonate (D), and TPP_{11}−malonate (E).

membrane potential ($\Delta\psi_m$) across the IMM (140−180 mV negative inside) is exploited by the TPP cation and uptake occurs according to the Nernst equation; hence, there is a 10-fold accumulation per ~60 mV of $\Delta\psi_m$.[4,12] While the positive charge on the phosphorus atom favors its accumulation into mitochondria in a Nernstian fashion, it also presents a problem when partitioning into the hydrophobic mitochondrial membrane. This is due to the large activation energy needed to remove the aqueous solvation shell for movement of the ion into the hydrophobic membrane core (Born energy).[12,20] Image forces and dipole interactions with the phospholipid esters also hinder TPP uptake; however, these contribute far less than the Born energy.[12,20] By introducing hydrophobic phenyl groups, the charge is spread over a larger area, and steric hindrance distances the water molecules from the charge; thus, the solvent-accessible charge is lower, and the free energy required to remove water molecules for partitioning into the membrane is reduced.[12,21]

Usually the drug or probe for delivery to mitochondria is permanently attached to the TPP cation.[16,18,22−24] However, a permanent attachment is not always appropriate, as the bulky TPP moiety may interfere with the biological activity of the molecule. To overcome this, the TPP can be conjugated to its cargo by a cleavable linker, enabling the small molecule to remain in the organelle while the TPP delivery module redistributes. This approach has been used to deliver lipoic

https://dx.doi.org/10.1021/acs.molpharmaceut.0c00533
Mol. Pharmaceutics 2020, 17, 3526−3540

acid to mitochondria by attaching it via an ester link that was cleaved within mitochondria by an endogenous esterase, which was proposed to be aldehyde dehydrogenase 2 (ALDH2).[25] Additionally, an *S*-nitrosothiol was attached to TPP, which was reduced within mitochondria, releasing nitric oxide.[8,26] There are many small bioactive molecules, including key mitochondrial substrates, that contain two carboxylic acid functions whose biological activity would be blocked by conjugation to TPP. Therefore, here, we set out to develop a cleavable TPP vector to deliver bioactive dicarboxylates to mitochondria.

One approach to deliver dicarboxylic acids to mitochondria is by linking one carboxylic acid to TPP by a cleavable ester, while also masking the other carboxylate as an ester to neutralize the carboxylate's negative charge at biological pH values. However, even though its mitochondrial accumulation may be favorable, the two ester bonds required to be cleaved to release the active compound would have different hydrolysis properties and thus create uncertainty in drug delivery. Instead, we focused on linking the dicarboxylate to TPP by a single ester, while leaving the other carboxylate free (Figure 1A). In addition to requiring only a single ester cleavage, this approach may enhance the overall mitochondrial uptake (~4−10 fold) because the uptake of weak acids, such as carboxylates, into mitochondria is favored by the pH gradient between the cytosol (pH ~7.2) and mitochondrial matrix (pH ~8).[27,28] This suggests that a dicarboxylate attached to a TPP cation by a single ester linkage should effectively deliver a dicarboxylate to mitochondria (Figure 1A); however, it is unclear if this approach would be effective in cells or *in vivo*.

To assess this targeting strategy, we chose the simple dicarboxylate malonate as our test compound. In addition to being chemically simple, malonate is a competitive inhibitor of succinate dehydrogenase (SDH)[29,30] and can inhibit the succinate-driven production of reactive oxygen species (ROS) by reverse electron transfer (RET) through mitochondrial complex I.[31,32] This production of ROS is dependent on succinate availability to SDH, which can be prevented by the delivery of malonate, enabling this delivery to be assessed.[31,33] We found that this mitochondria-targeted strategy could deliver malonate to mitochondria, provided that the linker between TPP and malonate was hydrophobic enough to counteract the polarity of the free carboxylic acid and thus enable membrane permeation. Here, we show that a TPP−undecyl monoester of malonic acid (TPP_{11}−malonate) accumulated in mitochondria in response to the proton motive force, releasing malonate within mitochondria in cells and *in vivo*. Thus, we have established a general procedure for the selective and enhanced delivery of dicarboxylates to mitochondria in cells and *in vivo*.

EXPERIMENTAL SECTION

Materials. Cell culture materials (Gibco branded) were purchased from Thermo Fisher Scientific. All other materials were purchased from Sigma-Aldrich, unless otherwise stated.

Synthesis of TPP−Malonate Monoesters. Detailed chemical synthesis of the TPP−malonate monoesters is provided in the Supporting Information.

Maintenance of Cells in Culture. C2C12 and HeLa cells were obtained from American Type Culture Collection (ATCC). Both were maintained at 37 °C, 5% CO_2 and 100% humidity in DMEM media (4.5 g/L of glucose, 1 mM sodium pyruvate, 2 mM Glutamax, 1.5 g/L of sodium bicarbonate) supplemented with 10% Fetal Bovine Serum (FBS), 100 U/mL of penicillin and 100 mg/mL of streptomycin.

Animals. All procedures were carried out in accordance with the United Kingdom (UK) Animals (Scientific Procedures) Act of 1986 and the University of Cambridge Animal Welfare Policy under project licenses 70/8702, 70/8238, and 70/7963, reviewed by the University of Cambridge Animal Welfare Ethical Review Board. Wistar rats (female, 10−12 weeks, ~250 g) and C57BL/6J mice (male, 8−12 weeks, ~25 g) were obtained from Charles River Laboratories UK (Margate, UK). Both were maintained with *ad libitum* access to laboratory chow and water. Animals were culled by cervical dislocation with accordance to UK Home Office Schedule 1 procedures.

Isolation of Rat Liver and Heart Mitochondria. Rat heart and liver mitochondria were isolated as described previously.[16,34] Briefly, the tissue was washed with STE buffer (250 mM sucrose, 5 mM Tris-Cl, 1 mM EGTA; pH 7.4, 4 °C) or STEB buffer for hearts (STE + 0.1% (w/v) bovine serum albumin (BSA)) and minced finely. The minced tissue was homogenized in a Dounce homogenizer in the relevant buffer and centrifuged (1000 *g*, 5 min, 4 °C). The resulting supernatant (for hearts, the supernatant was filtered through pre-wet muslin) was centrifuged to pellet mitochondria (10000 *g*, 10 min, 4 °C). The mitochondrial pellet was resuspended in buffer and recentrifuged under the same conditions to pellet mitochondria, and the process was repeated. The final mitochondrial pellet for all tissues was resuspended in STE buffer (no BSA) and assayed for the protein concentration by a bicinchoninic acid (BCA) assay (Thermo Fisher Scientific, UK).

Preparation of Bovine Heart Mitochondrial Membranes. Bovine heart mitochondria were isolated by differential centrifugation, as described previously.[35] To prepare membranes, bovine heart mitochondria were blended with Milli-Q water (4 °C) before adding KCl (150 mM final concentration) and were further blended until homogeneous. The suspension was centrifuged (13500 *g*, 40 min, 4 °C), the pellet homogenized in resuspension buffer (20 mM Tris-Cl, 1 mM EDTA, 10% (v/v) glycerol, pH 7.55 at 4 °C), and protein concentration determined by a BCA assay.

Measuring Complex II + III Activity. Complex II + III activity was measured as described previously.[36] Bovine heart mitochondrial membranes (80 μg of protein/mL) were incubated in potassium phosphate buffer (50 mM potassium phosphate, 1 mM EDTA, pH 7.4, 4 °C) supplemented with KCN (3 mM), rotenone (4 μg/mL), and succinate. In a 96-well microplate, compounds and a membrane incubation solution were plated and incubated (15 min, 37 °C) ± porcine liver esterase (PLE; 1 mg of protein/mL). Oxidized cytochrome c was added prior to measuring the respiratory chain activity by following the reduction of cytochrome c spectrophotometrically at 550 nm (20 s intervals for 5 min, 30 °C; Spectramax Plus 384, Molecular Devices, UK). Final concentrations of bovine heart mitochondrial membranes (10 μg of protein/well), cytochrome (30 μM), inhibitor (100 μM), and succinate (1 mM) were used.

LC-MS/MS Analysis of Malonate. LC-MS/MS measurement of malonate was performed using an LCMS-8060 mass spectrometer (Shimadzu, UK) with a Nexera UHPLC system (Shimadzu, UK), as described previously.[31] Samples were stored in a refrigerated autosampler (4 °C) until injection of 5 μL into a 15 μL flowthrough needle. A SeQuant ZIC-HILIC

https://dx.doi.org/10.1021/acs.molpharmaceut.0c00533
Mol. Pharmaceutics 2020, 17, 3526−3540

column (3.5 μm, 100 Å, 150 × 2.1 mm, 30 °C column temperature; Merck Millipore, UK) with a ZIC-HILIC guard column (200 Å, 1 × 5 mm) was used for liquid chromatography. A flow rate of 0.2 mL/min was used with mobile phases of (A) 10 mM ammonium bicarbonate (pH unchanged) and (B) 100% acetonitrile. A gradient of 0−0.1 min, 80% MS buffer B; 0.1−4 min, 80−20% MS buffer B; 4−10 min, 20% MS buffer B; 10−11 min, 20−80% MS buffer B; and 11−15 min, 80% MS buffer B was used. The mass spectrometer was operated in negative ion mode with multiple reaction monitoring (MRM), and spectra were acquired using Labsolutions software (Shimadzu, UK), with malonate levels calculated from a standard curve in MS extraction buffer (50% (v/v) methanol, 30% (v/v) acetonitrile, and 20% (v/v) MS-grade water) compared to 1 nmol of MS internal standard ($^{13}C_3$-malonate).

LC-MS/MS Analysis of TPP−Malonate Monoesters. For TPP−malonate monoesters, separation was achieved using an I-class Acquity ultra-performace liquid chromatography (UPLC) ethylene bridge hybrid (BEH) C18 column (1 × 50 mm, 1.7 μm; Waters, UK) with a Waters UPLC filter (0.2 μm; Waters, UK). A flow rate of 150 μL/min was used with mobile phases of (C) 0.1% (v/v) formic acid in 100% water and (D) 0.1% (v/v) formic acid in 100% acetonitrile. A gradient of 0−0.3 min, 5% D; 0.3−3 min, 5−100% D; 3−4 min, 100% D; 4.0−4.10 min, 100−5% D; 4.10−6.00 min, 5% D was used. The mass spectrometer was operated in the positive ion mode with multiple reaction monitoring (MRM), and spectra were acquired using Labsolutions software (Shimadzu), with compound quantities calculated from relevant standard curves in MS extraction buffer compared to a 100 pmol MS internal standard (d_{15}-3-OH propyl-TPP).

RP-HPLC-UV Analysis of TPP−Malonate Monoesters. RP-HPLC-UV was used for the characterization of TPP-linked compounds, as described previously.[37] Samples were prepared in 1 mL volumes in 25% (v/v) acetonitrile + 0.1% (v/v) trifluoroacetic acid (TFA) and filtered using a 0.22 μm syringe-driven filter unit (Merck Millipore, UK). Then, 800 μL of filtrate was loaded into a 2 mL sample loop, and compounds were separated using a Jupiter 300 Å C18 RP-HPLC column (Phenomenex, UK) attached to a Widepore C18 guard column (Phenomenex, UK) using a Gilson 321 pump (Gilson, UK). Compounds were eluted using a gradient elution with a mobile phase composition consisting of HPLC buffer (A) 0.1% (v/v) trifluoroacetic acid (TFA) in water and HPLC buffer (B) 0.1% (v/v) TFA in acetonitrile. Compounds were eluted at a flow rate of 1 mL/min with a gradient of 0−2 min, 5% B; 2−17 min, 5−100% B; 17−19 min, 100% B; and 19−22 min, 100−5% B, and the UV absorbance was detected at 220 nm with a Gilson 151 UV−vis spectrophotometer (Gilson, UK).

Hydrolysis of TPP−Malonate Monoesters. TPP−malonate monoesters (200 μM) and the internal standard (IS; isoamyl-TPP or propyl-TPP; 200 μM) were incubated in KCl buffer (120 mM KCl, 10 mM 4-(2-hydroxyethyl)-1-piperazineethanesulfonic acid (HEPES), 1 mM ethylene glycol-bis(β-aminoethyl ether)-*N*,*N*,*N*′,*N*′-tetraacetic acid (EGTA); pH 7.2 or 8, 37 °C) on a shaking heatblock (1000 rpm; Eppendorf, UK). Then, 20 μL samples were taken at time points of 0, 1, 2, 4, 8, and 24 h; extracted in 250 μL of HPLC buffer B; diluted with 750 μL of HPLC buffer A; and filtered and analyzed by UV-HPLC. For enzymatic hydrolysis, the KCl buffer (pH 7.2) was supplemented with porcine liver esterase (1 mg of protein/mL), and additional time points at 15 and 30 min were taken.

Mitochondrial Uptake of TPP−Malonate Monoesters. Rat liver (RLM) or heart (RHM) mitochondria (0.5 mg of protein/mL) were incubated in 2 mL of KCl buffer (pH 7.2, 37 °C) supplemented with TPP−malonate monoesters and an internal control (propyl-TPP or isoamyl-TPP to avoid retention time overlap) (5 μM each) in a shaking heatblock (1000 rpm; Eppendorf, UK). Mitochondria were energized with glutamate and malate (5 mM each). The uptake was assessed at 5, 10, and 15 min of incubation. Where 2-[2-[4-(trifluoromethoxy)phenyl]hydrazinylidene]-propanedinitrile (FCCP) (1 μM), nigericin (100 nM) or tetraphenylborate (5 μM) were used, these were added at the beginning of the 5 min incubations. After an appropriate incubation time, samples were rapidly cooled on ice before pelleting mitochondria by centrifugation (10000 *g*, 5 min, 4 °C). Then, 750 μL of the supernatant was extracted in 250 μL of HPLC buffer B and filtered and analyzed by UV-HPLC. The mitochondrial pellet was dried with tissue paper and extracted with 250 μL of HPLC buffer B while vortexing, and then centrifuged (17000 *g*, 10 min, 4 °C). The resulting supernatant was diluted with 750 μL of HPLC buffer A and filtered before analyzing by UV-HPLC.

Measurement of H_2O_2 Production in Isolated Heart Mitochondria. ROS production by RET was measured by following the conversion of Amplex Red to resorufin. Isolated RHM were incubated in a KCl buffer supplemented with Amplex Red (12.5 μM; Invitrogen, Thermo Fisher Scientific), BSA (200 μg/mL), superoxide dismutase (40 μg/mL), horseradish peroxidase (20 μg/mL), succinate (5 mM), and compound (10 μM) or rotenone (4 μg/mL) in a 96-well plate. Resorufin fluorescence was detected by λ_{ex}= 570 nm and λ_{em}= 585 and calibrated against known concentrations of hydrogen peroxide (46.6 M^{-1} cm^{-1} at 240 nm).

Incubation of Cells with TPP−Malonate Monoesters. C2C12 or HeLa cells were plated in 6-well plates (300000 cells/well) and adhered overnight. The following day, the cell culture medium was replaced with fresh medium (DMEM + 10% FBS) containing TPP_{11}−malonate (10 μM) and incubated for 0−240 min prior to extracting. Parallel plates were incubated under the same conditions and used to determine protein levels by a BCA assay (Thermo Fisher Scientific, UK).

After incubation, cells and supernatant were extracted for LC-MS/MS analysis. The supernatant was removed and centrifuged (17000 *g*, 10 min, 4 °C) before adding 50 μL of the resulting supernatant to 750 μL of a MS extraction buffer (50% (v/v) methanol, 30% (v/v) acetonitrile, and 20% (v/v) water) containing a MS internal standard (1 nmol $^{13}C_3$-malonate and 100 pmol d_{15}-3-OH propyl-TPP). Cells were washed 4 times with ice-cold PBS before 500 μL of the MS extraction buffer containing the MS internal standard was added to each well and incubated for 15 min on dry ice. Cells were scraped into microcentrifuge tubes and, together with the supernatant samples, were agitated (1200 rpm, 15 min, 4 °C) before incubating at −20 °C for 1 h. Samples were centrifuged twice to remove pelleted debris (17000 *g*, 10 min, 4 °C), and the resulting supernatant was analyzed by LC-MS/MS.

***In Vivo* Delivery of TPP_{11}−Malonate Monoester.** TPP_{11}−malonate (1.6 mg/kg) was administered to C57BL/6J mice via a 100 μL tail vein bolus injection in 0.9% saline. Mice were culled either 5 or 40 min after injection, and the

https://dx.doi.org/10.1021/acs.molpharmaceut.0c00533
Mol. Pharmaceutics 2020, 17, 3526−3540

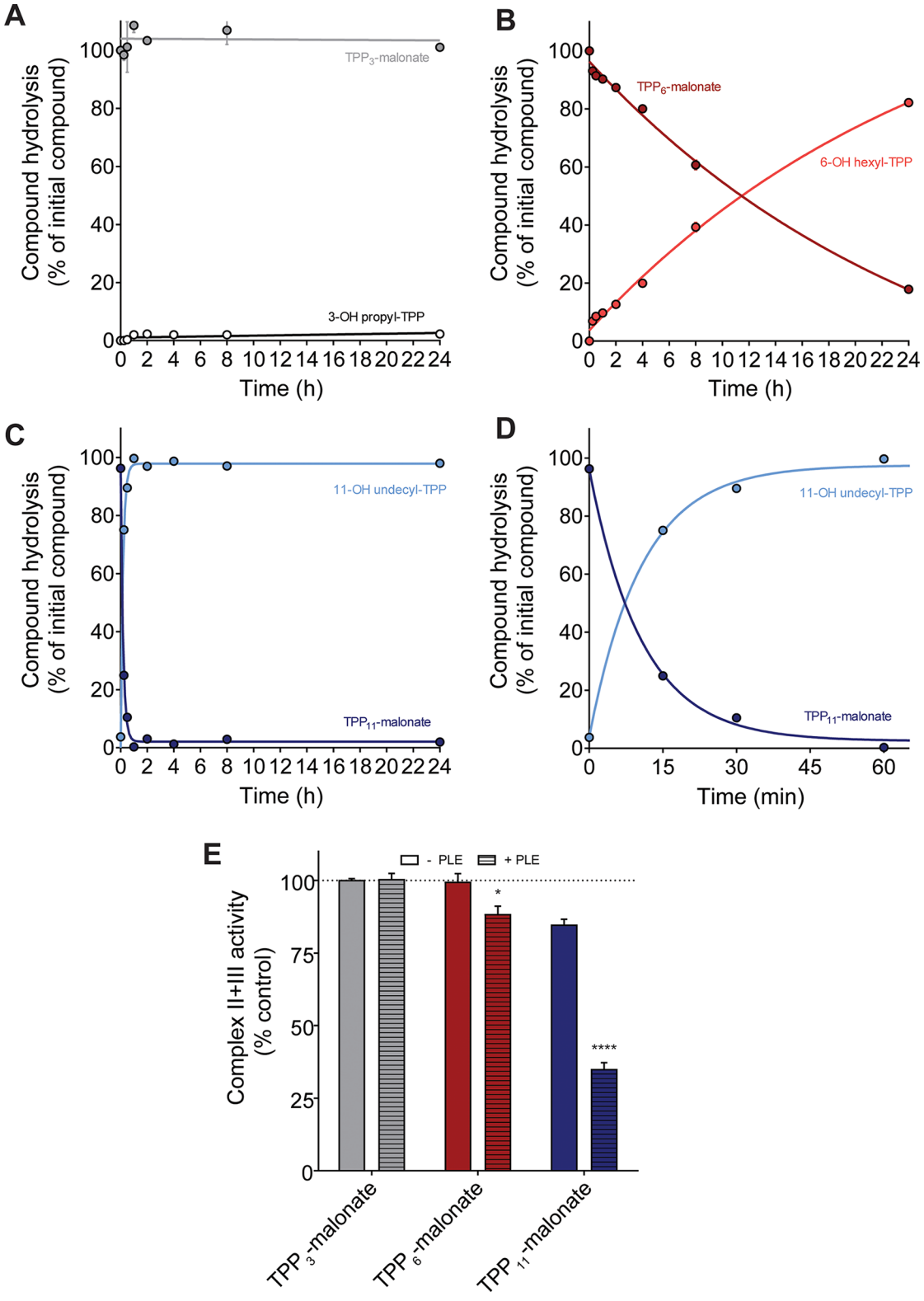

Figure 2. Malonate release from TPP−malonate monoesters. (A−D) TPP−malonate monoesters and internal control (isoamyl-TPP for TPP_3 and TPP_6−malonate or propyl-TPP for TPP_{11}−malonate) were incubated in the KCl buffer with PLE (1 mg of protein/mL) for up to 24 h and TPP-containing compounds measured by RP-HPLC-UV at 220 nm. Peak areas from each sample were normalized to the peak area of the internal control and presented as a percentage of the peak area of the initial parent compound (mean ± SEM, $n = 3$). An expanded view of early time points of the TPP_{11}−malonate incubation from panel C is presented in panel D. (E) SDH inhibition by TPP−malonate monoesters. BHMMs (80 μg of protein/mL) were incubated with the vehicle control (0.1% EtOH) or TPP−malonate monoesters (100 μM) ± PLE (1 mg of protein/mL) with succinate (1 mM) for 15 min before measuring complex II + III activity by observing the reduction of ferricytochrome c (30 μM) spectrophotometrically at 550 nm (mean ± SEM % of vehicle control activity, $n = 3$). The statistical significance was assessed by two-way ANOVA with Tukey's correction for multiple comparisons (between +PLE and −PLE), where *$p < 0.05$ and ****$p < 0.0001$.

https://dx.doi.org/10.1021/acs.molpharmaceut.0c00533
Mol. Pharmaceutics 2020, 17, 3526−3540

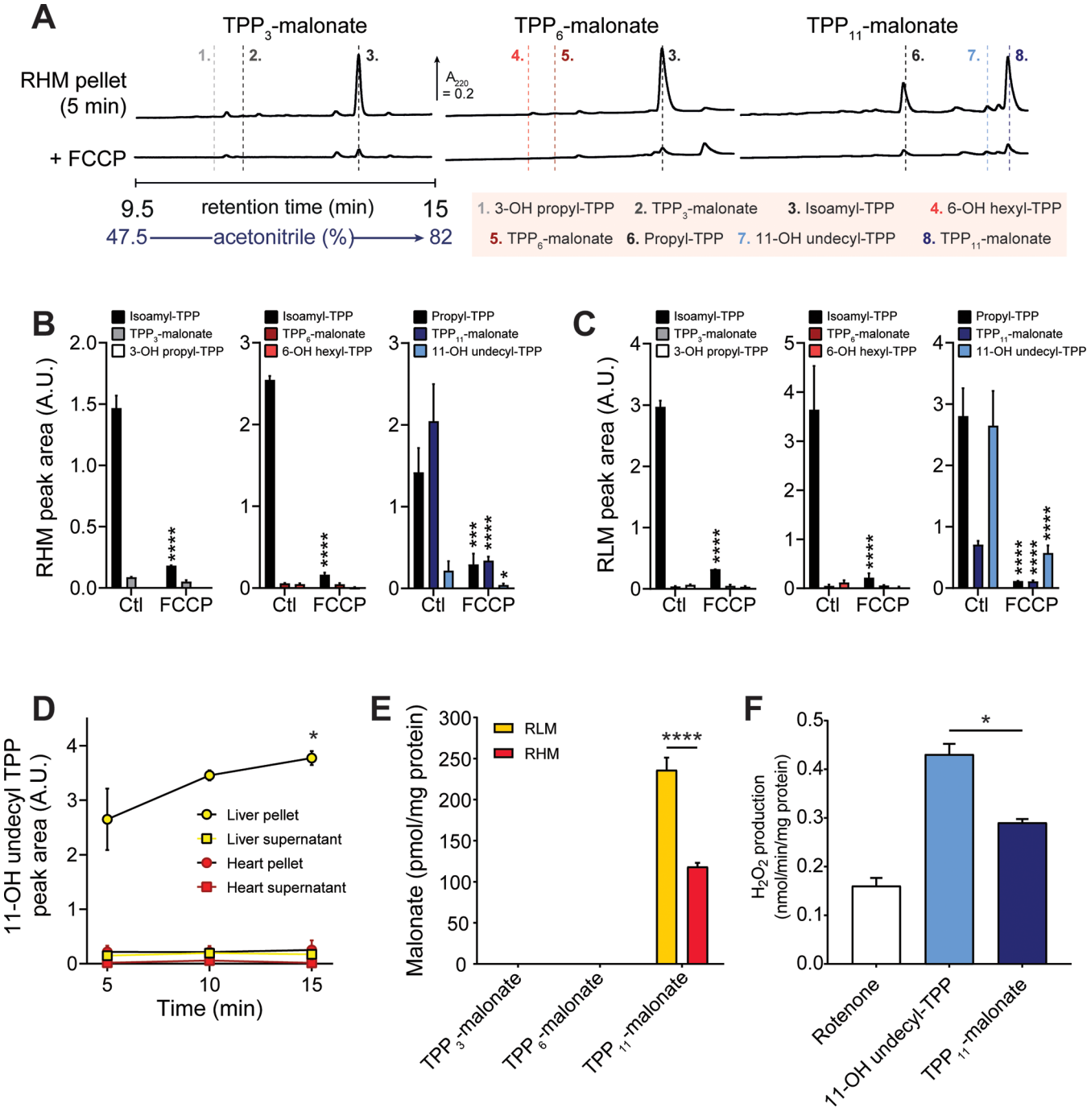

Figure 3. Mitochondrial accumulation and malonate delivery by TPP−malonate monoesters. TPP−malonate monoesters (5 μM) and internal control (5 μM; isoamyl-TPP for TPP_3− and TPP_6−malonate or propyl-TPP for TPP_{11}−malonate to avoid retention time overlap) were incubated with energized RLM or RHM (0.5 mg of protein/mL) ± FCCP (1 μM) before pelleting mitochondria, extracting the pellet and supernatant, and analyzing by RP-HPLC-UV at 220 nm. (A) Representative RP-HPLC-UV traces of TPP−malonate monoesters in pelleted rat heart mitochondria of 3 biological replicates. (B−C) Quantification of TPP-containing species peak areas in the mitochondrial pellet of (B) RHM and (C) RLM (mean ± SEM, n = 3). Statistical significance was assessed by two-way ANOVA with Dunnett's correction for multiple comparisons (compared to the relevant control group), where *p < 0.05, ***p < 0.001, and ****p < 0.0001. (D) 11-OH undecyl-TPP levels in the mitochondrial pellet or supernatant after 5, 10, or 15 min of incubation with TPP_{11}−malonate. (E) Mitochondrial malonate delivery. The energized RLM or RHM (0.5 mg of protein/mL) were incubated with TPP−malonate monoesters (10 μM) for 5 min before analyzing the mitochondrial pellet malonate levels by LC-MS/MS (mean ± SEM, n = 3). The statistical significance was assessed by two-way ANOVA with Bonferroni's correction for multiple comparisons, where ****p < 0.0001. (F) Inhibition of ROS production from RET by TPP−malonate monoesters. RHM were incubated with mitochondria-targeted malonate monoesters (10 μM) or rotenone (0.5 μM; rotenone inhibits mitochondrial complex I, thus abolishing RET), and RET was initiated by the addition of succinate (5 mM). ROS from RET were measured as the conversion of Amplex Red to resorufin by fluorescence at excitation at 570 nm and emission at 580 nm. H_2O_2 production from RET was measured by interpolation from a H_2O_2 standard curve under the same conditions (mean ± SEM, n = 3). The statistical significance was assessed by one-way ANOVA with Dunnett's correction for multiple comparisons, where *p < 0.05.

https://dx.doi.org/10.1021/acs.molpharmaceut.0c00533
Mol. Pharmaceutics 2020, 17, 3526−3540

organs were harvested and snap frozen in liquid nitrogen. TPP-containing compounds and malonate were extracted from tissues by homogenizing tissue (40 mg of wet weight/mL) in the MS extraction buffer containing the MS internal standard (1 nmol of $^{13}C_3$-malonate and 100 pmol of d_{15}-3-OH propyl-TPP) in a Precellys 24 tissue lyser (6500 rpm, 15 s × 2; Bertin Instruments, France) using CK-28R homogenizing tubes (Bertin Instruments, France). Homogenized samples were stored at −20 °C for 1 h before being centrifuged twice to remove the pelleted debris (17000 *g*, 10 min, 4 °C), and the resulting supernatant was analyzed by LC-MS/MS.

Statistical Analysis, Randomization, and Blinding. Data in figures are presented as the mean ± standard error of the mean (SEM) unless indicated in the figure legend. The statistical analysis was assessed by one- or two-way ANOVA followed by the appropriate *post hoc* correction for multiple comparisons or, where two groups were assessed, an unpaired two-tailed Student's *t* test. A p value <0.05 was considered significant. Statistics were calculated in Prism 8.4 software (Graphpad Software Inc., USA). Randomization and blinding were carried out where possible: *in vivo* samples were processed for extraction blindly, and all mass spectrometry samples were randomized and analyzed blindly.

Data Availability. The data corresponding to the synthesized compounds are available at 10.5525/gla.researchdata.1031. Data supporting the findings in this study will be made available upon reasonable request to the corresponding authors.

RESULTS

TPP−Malonate Monoester Prodrugs for Mitochondrial Delivery. The delivery of dicarboxylate molecules to mitochondria is of interest due to their central role in metabolism and their contribution to many pathologies.[1−3] While endogenous transport mechanisms for dicarboxylates exist, these are limited by substrate specificity and thus may be unsuitable for rationally designed small molecule dicarboxylate drugs. Furthermore, to achieve mitochondrial delivery, two endogenous uptake mechanisms must be present and also facilitate rapid uptake into mitochondria, without metabolism of the drug in the cytosol. To overcome this, we thought to conjugate a small molecule dicarboxylate to the TPP mitochondria-targeting moiety to overcome the many biological barriers to the delivery of dicarboxylates.

Previous work had shown that TPP-linked weak acids have increased mitochondrial uptake due to their steady-state accumulation being driven by both the membrane potential and pH gradient between the cytosol and mitochondrial matrix (Figure 1A).[27,28] Although the carboxylic acid enhances endpoint uptake, it decreases the membrane permeability and thus the rate of uptake. Therefore, to enable the mitochondrial uptake, any TPP conjugate that includes a carboxylic acid will likely need increased overall hydrophobicity to counteract the polarity of its carboxylic acid group.[27,28] Therefore, we synthesized three TPP−malonate monoesters with a range of hydrophobicities using alkyl linkers of increasing lengths: propyl, hexyl, and undecyl (TPP_3−malonate, TPP_6−malonate, and TPP_{11}−malonate, respectively) (Figures 1B and S1). Each molecule contained an ester bond attaching the TPP linker to malonate, which once hydrolyzed should release malonate and its corresponding TPP alcohol (Figure 1C−E).

Hydrolysis of TPP−Malonate Monoesters *In Vitro*. Using a RP-HPLC method to detect the TPP−alcohol products of ester hydrolysis (Figure S2), we demonstrated that all the TPP−malonate monoesters were stable at pH 7.2 or 8 for up to 24 h (Figure S3). To test if the TPP−malonate monoesters could be cleaved enzymatically, we used porcine liver esterase (PLE), which is widely used as a surrogate for intracellular esterases.[38−40] The hydrolysis rates depended dramatically on the alkyl linker length (Figure 2A−D). While TPP_{11}−malonate was completely hydrolyzed by PLE within 1 h, it took 24 h to hydrolyze ∼80% of TPP_6−malonate, and the hydrolysis of TPP_3−malonate was negligible. As hydrolysis of the TPP−malonate monoesters should also release malonate, an inhibitor of SDH, we measured the effect of the compounds on the SDH activity of bovine heart mitochondrial membranes (BHMMs) treated with PLE. This showed that PLE treatment of TPP_{11}−malonate, and to a lesser extent TPP_6−malonate, could inhibit SDH activity but TPP_3−malonate could not (Figure 2E). The slight inhibitory effect of TPP_{11}−malonate in the absence of PLE is due to the interaction of the hydrophobic TPP compound with the membrane, as similarly seen with 11-OH undecyl-TPP alone (Figure S3G).[21,41]

The difference in the rate of hydrolysis between the three TPP−malonate monoesters is likely to be multifactorial. Steric hindrance from the bulky TPP moiety may contribute to the negligible hydrolysis of TPP_3−malonate.[42] However, steric hindrance alone is unlikely to explain the difference in hydrolysis between TPP_6−malonate and TPP_{11}−malonate and suggests that hydrophobic binding may also be a contributing factor.[43] Overall, this suggests an undecyl monoester of the dicarboxylate is favorable due to its more rapid enzymatic hydrolysis.

Uptake and Hydrolysis of TPP−Malonate Monoesters by Mitochondria. We next assessed if the malonate monoesters were accumulated by incubating the compounds with energized, isolated mitochondria. To do this, we pelleted the mitochondria and measured the uptake into the organelle of the TPP−malonate ester by RP-HPLC, in comparison to a simple alkyl-TPP molecule (either isoamyl-TPP or propyl-TPP, to avoid elution overlap) to confirm mitochondrial energization (Figures 3A and S4). A typical RP-HPLC trace from the incubation of the TPP_{11}−malonate monoester with rat heart mitochondria (RHM) is shown, which illustrates that both TPP_{11}−malonate and propyl-TPP were taken up by energized mitochondria and that this uptake was prevented by abolishing the membrane potential with the uncoupler FCCP (Figure 3A). Similar experiments showed that TPP_{11}−malonate was also accumulated by energized rat liver mitochondria (RLM) but that neither TPP_3−malonate nor TPP_6−malonate were accumulated by energized mitochondria (Figure S4A and B). Small differences in the levels of accumulation between liver and heart mitochondria likely reflect the differences in composition and volume between mitochondria from different tissues and cell types.[44] An analysis of the supernatant after pelleting the mitochondria showed that while TPP_{11}−malonate was taken up into the mitochondria, TPP_3− and TPP_6−malonate remained in the supernatant (Figure S4B). Furthermore, the addition of the tetraphenylborate (TPB) lipophilic anion, which often facilitates the mitochondrial uptake of TPP cations,[12,45] had little effect on the uptake of TPP_3− or TPP_6−malonate, confirming a lack of accumulation in mitochondria (Figure S4C).

The quantification of the uptake of the esters into mitochondria is shown in Figure 3B and C. These findings

https://dx.doi.org/10.1021/acs.molpharmaceut.0c00533
Mol. Pharmaceutics 2020, 17, 3526−3540

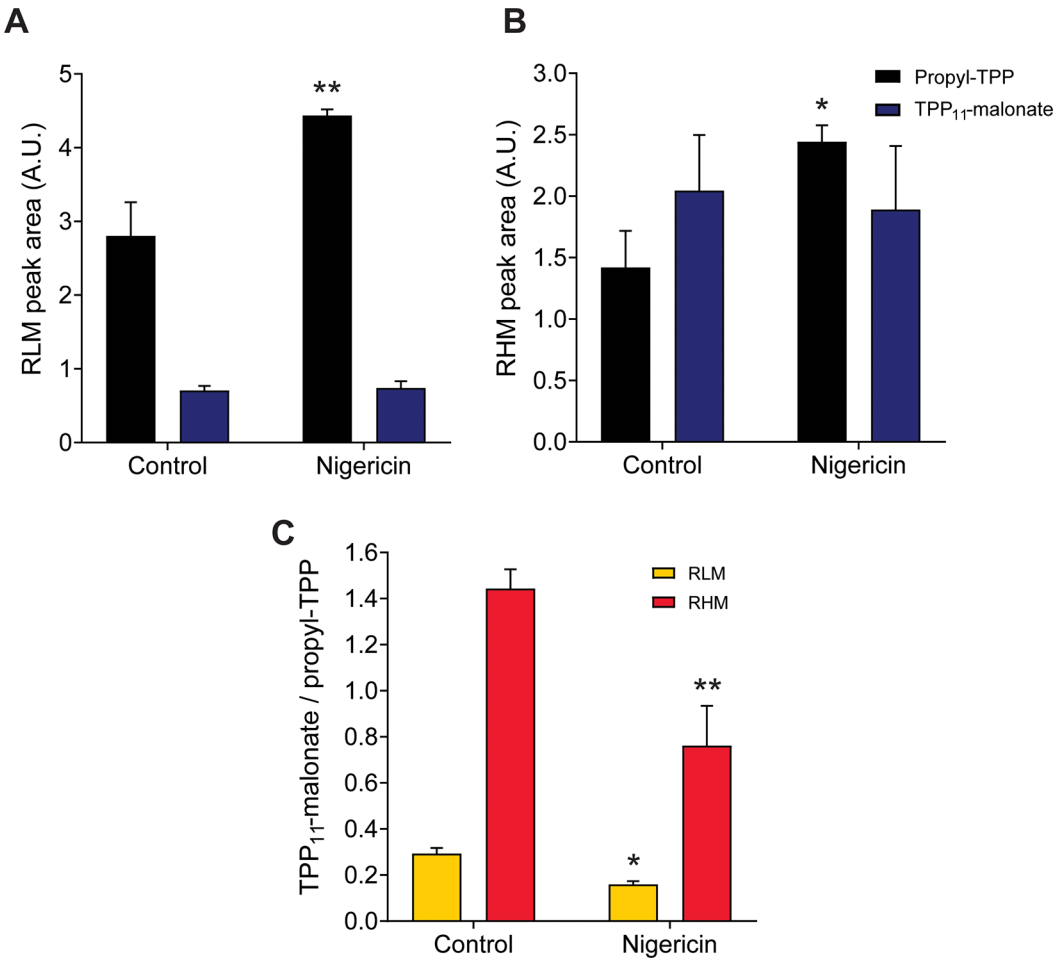

Figure 4. TPP_{11}−malonate mitochondrial accumulation is pH gradient-dependent. (A−C) Uptake of TPP_{11}−malonate ± nigericin (100 nM) in (A) RLM and (B) RHM. (C) Accumulation of TPP_{11}−malonate-derived compounds normalized to propyl-TPP ± nigericin. All data represent the mean ± SEM, $n = 3$. The statistical significance was assessed by two-way ANOVA with Dunnett's correction for multiple comparisons (compared to the relevant control group), where $*p < 0.05$.

are consistent with our earlier works, which showed that TPP cations linked to carboxylic acids required the incorporation of significant hydrophobicity to counteract the polarity of the carboxylic acid and enable membrane permeation.[27,28] We conclude that only TPP_{11}−malonate is accumulated by mitochondria due to its greater hydrophobicity.

In addition to TPP_{11}−malonate, its hydrolysis product 11-OH undecyl-TPP was also detected in mitochondria, and its level increased over time in RLM (Figures 3D and S4). At the same time, the amount of 11-OH undecyl-TPP in the supernatant was relatively unchanged (Figures 3D and S4). In heart mitochondria, where the esterase activity is lower (both contaminating and intramitochondrial),[46] a large accumulation of TPP_{11}−malonate occurs (peak 8 in Figures 3A and S4A), but the levels of its hydrolysis product, 11-OH undecyl-TPP (peak 7 in Figures 3A and S4A), in the mitochondrial pellet are far lower than in liver mitochondria (Figures 3D and S4).

We next measured the release of malonate within mitochondria incubated with TPP−malonate monoesters. Only TPP_{11}−malonate released malonate within mitochondria, consistent with its uptake by energized mitochondria (Figure 3E). That TPP_{11}−malonate uptake occurs before its hydrolysis is confirmed by the concentration of malonate observed in the mitochondrial pellet. Even if TPP_{11}−malonate was hydrolyzed to completion outside of mitochondria, the concentration of malonate in the supernatant would be 10 μM, a concentration that would lead to mitochondrial malonate levels less than 50 pmol/mg of protein,[31] far lower than the ∼250 pmol/mg of protein achieved by TPP_{11}−malonate (Figure 3E). TPP_{11}−malonate could deliver malonate intramitochondrially in both liver and heart mitochondria; however, the levels in heart mitochondria were significantly lower over these short-duration incubations, mirroring the lower hydrolysis within RHM (Figure 3E).

To test whether the malonate released from TPP_{11}−malonate could elicit the intended biological effect and inhibit SDH, we measured the production of the ROS hydrogen peroxide (H_2O_2), which is driven by SDH-dependent succinate oxidation and RET in isolated heart mitochondria (Figure 3F). TPP_{11}−malonate significantly reduced ROS production from succinate oxidation compared to equivalent concentrations of its cleaved products, 11-OH undecyl-TPP (Figure 3F) or malonate (Figure S4D), directly added to mitochondria. Thus, TPP_{11}−malonate significantly accumulates in mitochondria and hydrolyzes to release malonate, which subsequently inhibits SDH. As only TPP_{11}−malonate accumulated and hydrolyzed to release malonate in mitochondria, neither TPP_3−malonate nor TPP_6−malonate were tested in subsequent analyses.

https://dx.doi.org/10.1021/acs.molpharmaceut.0c00533
Mol. Pharmaceutics 2020, 17, 3526−3540

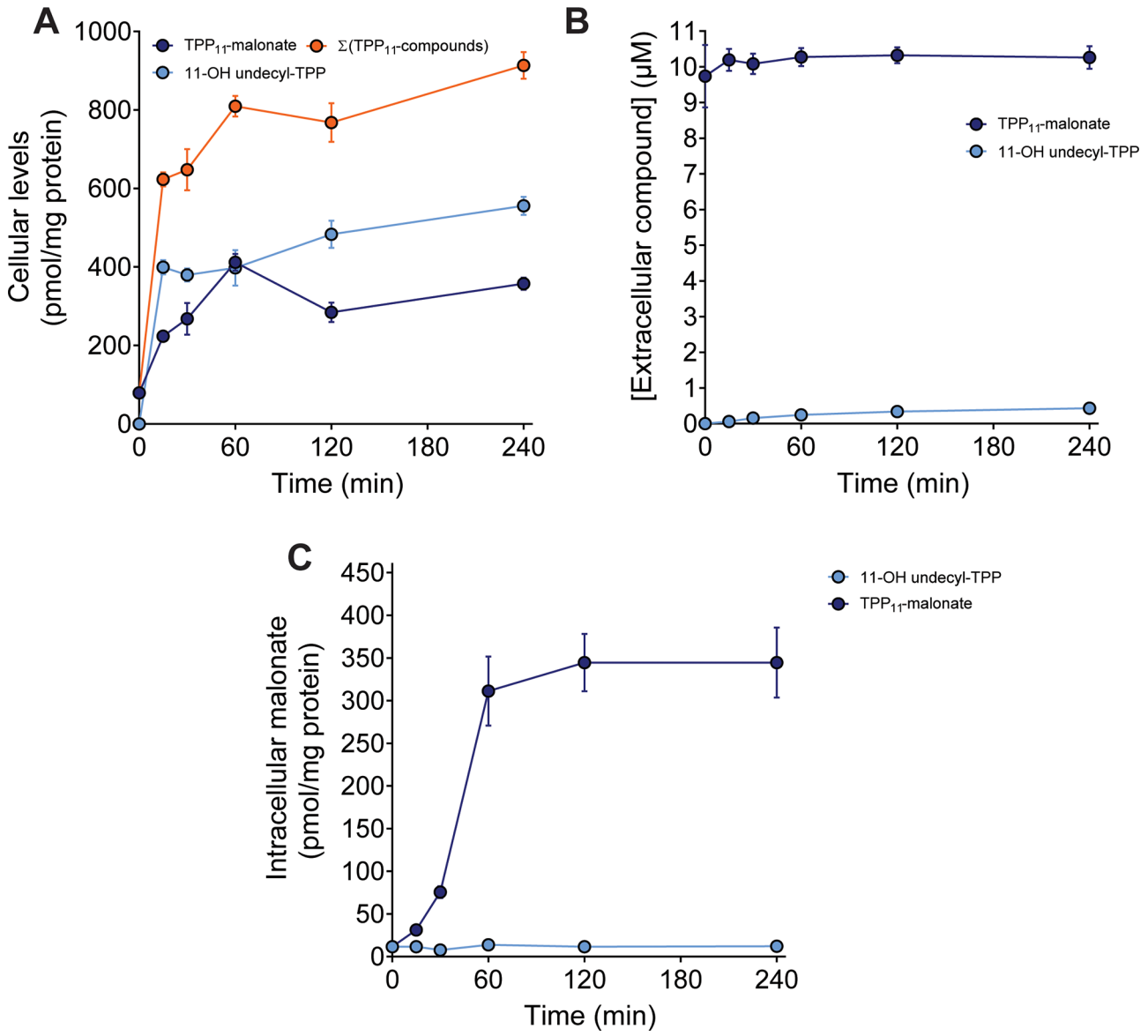

Figure 5. Malonate delivery by TPP_{11}−malonate in cells. (A−C) C2C12 cells were incubated with TPP_{11}−malonate (10 μM) before extraction of the cell pellet (A) and supernatant (B), and measurement of TPP-linked compounds (A and B) and malonate in the pellet (C) by LC-MS/MS (mean ± SEM, n = 3).

Uptake of TPP−Malonate Monoesters is Enhanced by the pH Gradient. We next explored whether the mitochondrial uptake of TPP_{11}−malonate was enhanced due to the interaction of the carboxylic acid with the pH gradient (Figure 1). To do this, we assessed its uptake by energized mitochondria in the presence of the K^+/H^+ exchanger nigericin, which will abolish the pH gradient across the mitochondrial inner membrane but increase the membrane potential.[47] The uptake of TPP_{11}−malonate was compared with the simple alkyl-TPP cation propyl-TPP as an internal control within the same incubation, which will only respond to changes in the membrane potential and will be unaffected by alterations in the pH gradient. Nigericin led to an increase in the uptake of propyl-TPP due to the elevated membrane potential but did not affect the uptake of TPP_{11}−malonate by RLM or RHM (Figure 4A and B). This lack of an effect of nigericin was likely due to the increased uptake of TPP_{11}−malonate due to the elevated membrane potential being balanced by the decrease in uptake due to the abolition of the pH gradient.[27,28] To test this possibility, we compared the ratio of the uptake of TPP_{11}−malonate to propyl-TPP in the presence of nigericin (Figure 4C). Normalizing the uptake of TPP_{11}−malonate to that of propyl-TPP enabled us to correct for the effects of membrane potential on uptake. Nigericin decreased the membrane potential-corrected uptake of TPP_{11}−malonate (Figure 4C). Therefore, the uptake of TPP_{11}−malonate is dependent on both the mitochondrial membrane potential and the pH gradients, similarly to other TPP-conjugated carboxylic acids,[27,28] and thus may increase its selectivity to mitochondrial delivery.

Uptake of TPP_{11}−Malonate by Cells and Release of Malonate. As TPP_{11}−malonate was an effective delivery vector in isolated mitochondria, we next assessed its effects in a cell model. We first exposed cells to a range of concentrations of TPP_{11}−malonate for 24 h and found no difference in the levels of cell death compared to a vehicle (EtOH) control (Figure S5A), suggesting that TPP−dicarboxylate esters can be safely used in cells without significant adverse effects. Next, to

https://dx.doi.org/10.1021/acs.molpharmaceut.0c00533
Mol. Pharmaceutics 2020, 17, 3526−3540

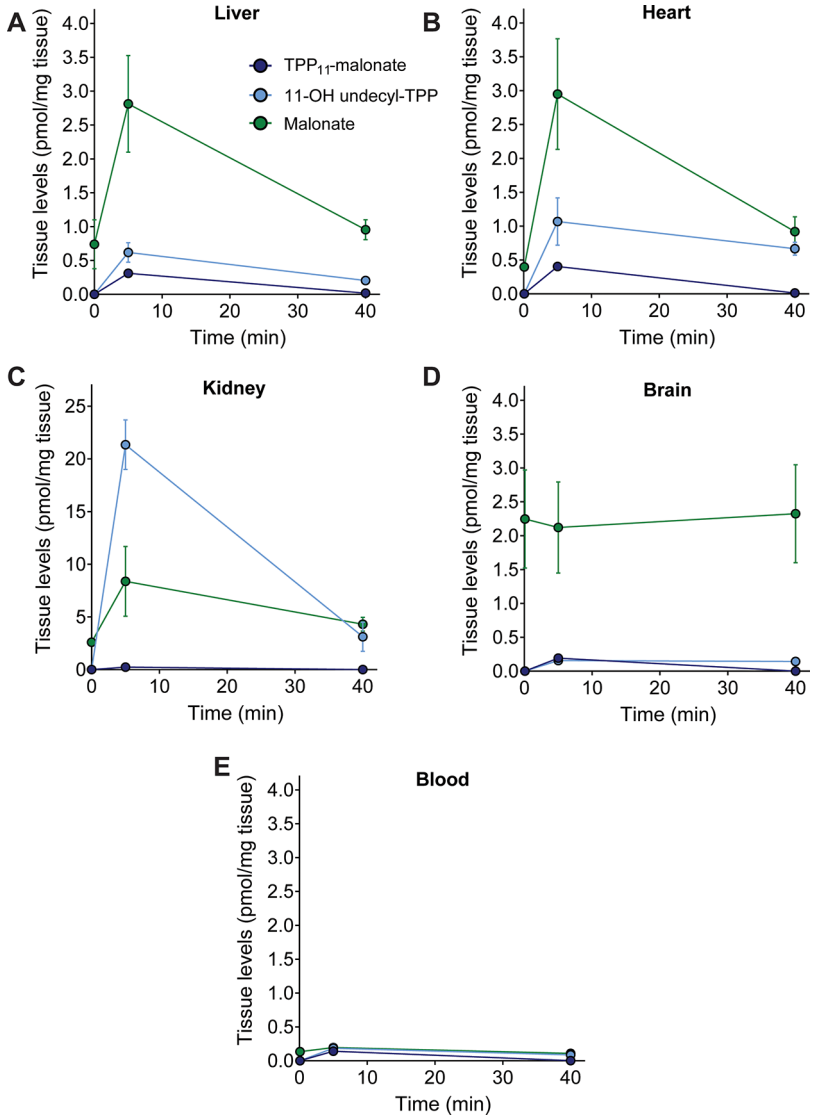

Figure 6. *In vivo* uptake of TPP_{11}–malonate. (A–E) C57BL/6J mice were tail-vein-injected with 1.6 mg/kg of TPP_{11}–malonate as a 100 μL bolus in 0.9% saline. Mice were culled and organs harvested 5 or 40 min after injection. The liver (A), heart (B), kidney (C), brain (D), and blood (E) were extracted and analyzed for TPP-linked compounds and malonate by LC-MS/MS (mean ± SEM, n = 3). The time "0" point values are from control, saline-injected animals.

assess the uptake of TPP_{11}–malonate and its hydrolysis in cells and *in vivo*, we set up a LC-MS/MS assay for both TPP_{11}–malonate and its hydrolysis product 11-OH undecyl-TPP (Figure S6). We incubated C2C12 mouse myoblasts with TPP_{11}–malonate for up to 4 h and measured the levels of the parent compound and hydrolysis products measured by LC-MS/MS in the cells and supernatant. The uptake of TPP_{11}–malonate into cells was rapid, with the compound found in the cell pellet even at the earliest time point possible (Figure 5A). The levels of TPP_{11}–malonate within cells increased over 1 h before plateauing. The hydrolysis product, 11-OH undecyl-TPP, mirrored TPP_{11}–malonate within the cellular pellet. This differed when HeLa cells were incubated with TPP_{11}–malonate, as the levels of TPP_{11}–malonate continued to rise but 11-OH undecyl-TPP plateaued (Figure S5B). TPP_{11}–malonate was stable to hydrolysis in the extracellular medium (Figure 5B), suggesting TPP_{11}–malonate is taken up and hydrolyzed within the cells.

In addition, the intracellular levels of malonate after TPP_{11}–malonate treatment were significantly elevated compared to cells treated with 11-OH undecyl-TPP alone; thus, TPP_{11}–malonate effectively delivers malonate to cells (Figure 5C). While the levels of malonate in mitochondria cannot be accurately measured directly, due to the extremely rapid redistribution of metabolites during mitochondrial isolation, previous work has shown the mitochondrial selectivity of TPP cations,[16,48] suggesting that the malonate delivered intracellularly is likely to be delivered within mitochondria. Furthermore, TPP_{11}–malonate could also affect cellular respiration, confirming that the compound was entering mitochondria in cells and inhibiting mitochondrial function (Figure S5C).

Uptake of TPP_{11}–Malonate *In Vivo*. Next, we investigated the usefulness of TPP esters as a dicarboxylate delivery strategy, by testing TPP_{11}–malonate *in vivo*. C57BL/6J mice were injected with a bolus of TPP_{11}–malonate (1.6 mg/kg) via the tail vein and killed either 5 or 40 min after injection, and

https://dx.doi.org/10.1021/acs.molpharmaceut.0c00533
Mol. Pharmaceutics 2020, 17, 3526–3540

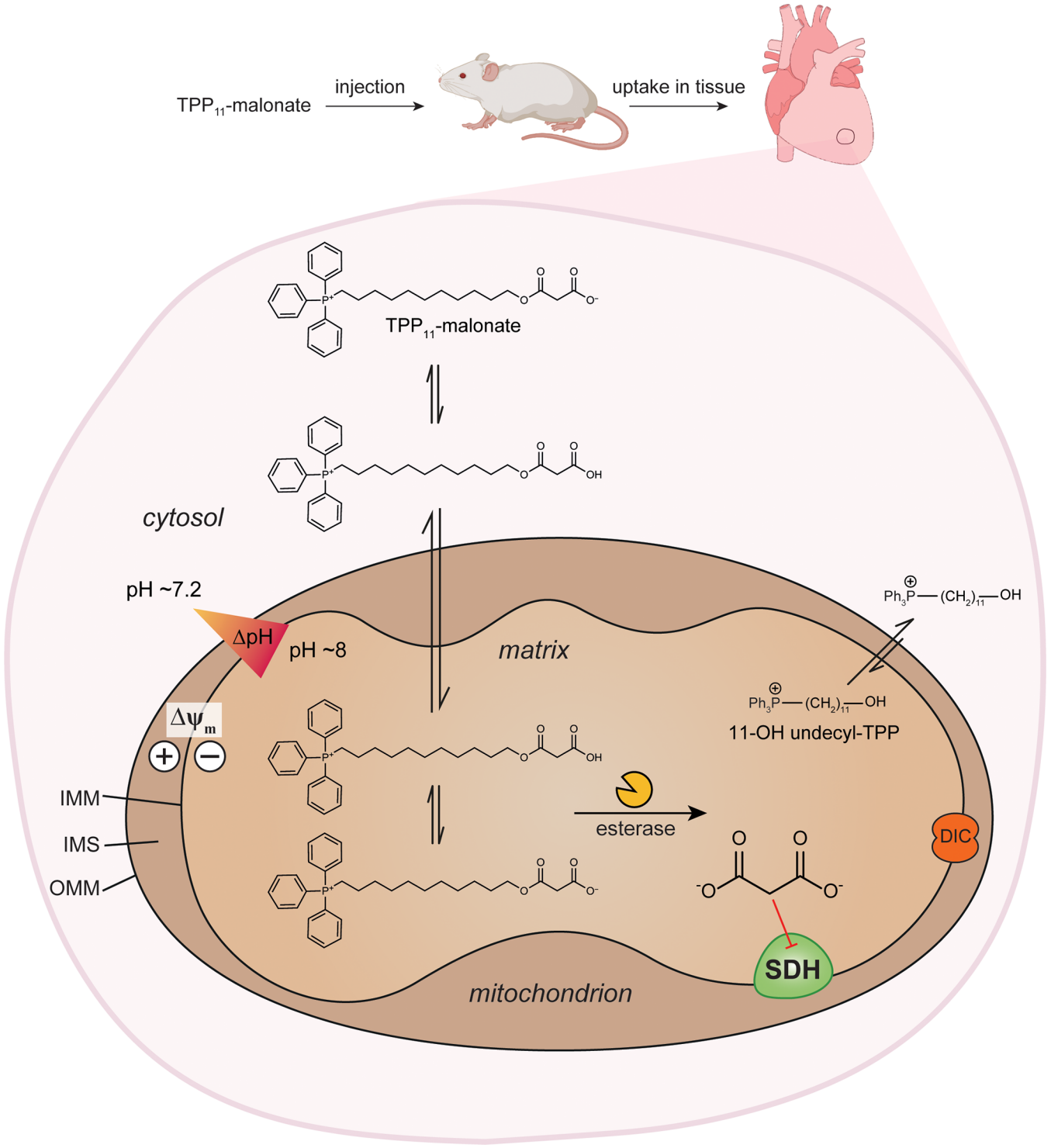

Figure 7. Schematic of TPP_{11}−malonate as a mitochondrial delivery strategy *in vivo*. Abbreviations: OMM, outer mitochondrial membrane; IMM, inner mitochondrial membrane; IMS, intermembrane space; SDH, succinate dehydrogenase; $\Delta\psi_m$, mitochondrial membrane potential; DIC, mitochondrial dicarboxylate carrier.

then, the tissues were snap frozen for later extraction and analysis by LC-MS/MS. TPP_{11}−malonate, 11-OH undecyl-TPP, and malonate were all detected in the analyzed tissues, with high levels 5 min after injection, which decreased 40 min after injection (Figure 6A−D). This suggests that TPP_{11}−malonate accumulated in different tissues, wherein it was hydrolyzed to release malonate within the mitochondria of the cells. The achieved levels of the compound were significantly higher in the kidney (Figure 6C) compared to the other tissues, suggesting a tissue distribution comparable to other TPP-linked compounds *in vivo*.[22,49] Furthermore, as the main route of clearance of TPP-linked compounds is via renal excretion,[22] this will also contribute to the accumulation of the TPP-linked compounds in the kidney. The blood levels of TPP_{11}−malonate and its hydrolysis products are low (Figure 6E), consistent with the rapid distribution of TPP-linked

https://dx.doi.org/10.1021/acs.molpharmaceut.0c00533
Mol. Pharmaceutics 2020, 17, 3526−3540

compounds from the circulation into tissues.[22,49] Overall, here we have developed a mitochondria-targeted malonate prodrug, which is able to deliver malonate selectively to mitochondria in cells and *in vivo* (Figure 7). This work confirms that a mitochondria-targeted prodrug approach is possible and facilitates the delivery and release of dicarboxylates within mitochondria.

DISCUSSION

Attaching a small molecule dicarboxylate to TPP led to a mitochondria membrane potential-dependent and pH gradient-dependent uptake for malonate as an example drug molecule. Due to the pK_a of malonate being particularly low (pK_{a1} = 2.83 and pK_{a2} = 5.69),[50] it provided challenging properties as a test cargo for the mitochondria-targeted delivery strategy. Despite this, TPP_{11}−malonate could deliver malonate in mitochondria of cells *in vitro* and *in vivo*. The use of an undecyl linker region facilitated uptake across biological membranes by increasing the hydrophobicity, which also enhanced ester hydrolysis. Finally, the elevated hydrophobicity may also increase the association of the compound with biological membranes, thereby increasing the compound's pK_a at the crossing site,[51] enhancing the rate of membrane permeation. These findings confirmed that the TPP_{11}-monoester is a viable approach for the delivery of dicarboxylates to mitochondria.

The shorter linker regions between malonate and the TPP moiety had a significant impact on the accumulation of the molecule across the mitochondrial inner membrane. Recent reports have shown that modifying the TPP-targeting group by replacing hydrogens in the phenyl groups with methyl groups (T^*PP^+) improves the efficiency of cation uptake into mitochondria.[52,53] Increasing the hydrophobicity, the solvent-accessible surface area and volume per charge (V_{pc}) of the cation improved accumulation into mitochondria.[20,52] The increase in linker length in our work also has the potential for increasing the solvent-accessible surface area and V_{pc} in addition to the increased hydrophobic interactions with the membrane; thus, the uptake of TPP_{11}−malonate with the increased linker regions is likely to be multifactorial. The complex biophysical interactions of TPP−dicarboxylate esters and biological membranes warrant further study in order to gain greater insight into their molecular characteristics and to aid future drug design.

TPP cations have been utilized previously to achieve selective mitochondrial accumulation of therapies and probes. However, their permanent conjugation to the bioactive molecule can present problems with hindering the drug's activity as well as promoting redistribution and potential removal from the cell due to the action of the TPP cation. Here, by conjugating the dicarboxylate to the TPP cation via a cleavable ester bond, the release of the bioactive compound in its native form is enabled, thus leaving its active site interaction unchanged. Furthermore, it enables the TPP-linker region to be metabolized and excreted independently of the bioactive drug. This has the potential added benefit of extending the exposure time of the drug without increasing the delivered dose or dose frequency.

By developing this cleavable mitochondria-targeting platform, this opens up the potential to selectively target particular isoforms of enzymes within mitochondria. As a number of enzymes within mitochondria are also found in the cytosol, differentiating the effects of a treatment with nontargeted dicarboxylate prodrugs may be challenging due to it acting upon both the cytosolic and mitochondrial forms. By attaching the active dicarboxylate compound via an ester bond to a TPP moiety, similarly to TPP_{11}−malonate, this would enable the assessment of the active compound's effect directly on mitochondria, with limited impact on the cytosolic isoform. Therefore, in addition to being a potential therapeutic platform, TPP−dicarboxylate esters may also be useful probe molecules to selectively uncover the roles of mitochondrial proteins within disease.

CONCLUSIONS

Mitochondria are central to the development of numerous pathologies. Mitochondria-targeted molecules have thus far led to insights into mitochondrial biology and new therapeutic approaches. Currently, a constraint on mitochondria-targeted molecules has been that the targeted molecule is permanently attached to the targeting platform, thus hindering activity within the mitochondria. Here, we have developed a mitochondria-targeted malonate monoester, which overcomes the problems described above by extensively accumulating in mitochondria, wherein it releases the cargo of interest. This suggests that further dicarboxylates could be delivered in a similar manner. Overall, we have shown that TPP−dicarboxylate monoesters are a promising strategy to deliver dicarboxylates selectively to mitochondria to investigate or treat mitochondria-related pathologies.

ASSOCIATED CONTENT

Supporting Information

The Supporting Information is available free of charge at https://pubs.acs.org/doi/10.1021/acs.molpharmaceut.0c00533.

Chemical synthesis; synthesis of TPP−malonate monoesters; base hydrolysis of TPP−malonate monoesters; nonenzymatic hydrolysis of TPP−malonate monoesters; uptake and hydrolysis of mitochondria-targeted malonate monoesters in rat liver and heart mitochondria; TPP_{11}−malonate incubation with cells; detection of TPP_{11}−malonate and 11-OH undecyl-TPP by LC-MS/MS; and supplementary methods (PDF)

AUTHOR INFORMATION

Corresponding Authors

Michael P. Murphy − *Molecular Research Center, Mitochondrial Biology Unit, Biomedical Campus and Department of Medicine, University of Cambridge, Cambridge CB2 0XY, United Kingdom*; Email: mpm@mrc-mbu.cam.ac.uk

Richard C. Hartley − *School of Chemistry, University of Glasgow, Glasgow G12 8QQ, United Kingdom*; orcid.org/0000-0003-1033-5405; Email: Richard.Hartley@glasgow.ac.uk

Authors

Hiran A. Prag − *Molecular Research Center, Mitochondrial Biology Unit, Biomedical Campus, University of Cambridge, Cambridge CB2 0XY, United Kingdom*; orcid.org/0000-0002-4753-8567

Duvaraka Kula-Alwar − *Department of Medicine, University of Cambridge, Cambridge CB2 0QQ, United Kingdom*

https://dx.doi.org/10.1021/acs.molpharmaceut.0c00533
Mol. Pharmaceutics 2020, 17, 3526−3540

Laura Pala − *School of Chemistry, University of Glasgow, Glasgow G12 8QQ, United Kingdom*
Stuart T. Caldwell − *School of Chemistry, University of Glasgow, Glasgow G12 8QQ, United Kingdom*
Timothy E. Beach − *Department of Surgery, Cambridge National Institute for Health Research Biomedical Research Centre, University of Cambridge, Cambridge CB2 0QQ, United Kingdom*
Andrew M. James − *Molecular Research Center, Mitochondrial Biology Unit, Biomedical Campus, University of Cambridge, Cambridge CB2 0XY, United Kingdom*
Kourosh Saeb-Parsy − *Department of Surgery, Cambridge National Institute for Health Research Biomedical Research Centre, University of Cambridge, Cambridge CB2 0QQ, United Kingdom*
Thomas Krieg − *Department of Medicine, University of Cambridge, Cambridge CB2 0QQ, United Kingdom*

Complete contact information is available at: https://pubs.acs.org/10.1021/acs.molpharmaceut.0c00533

Author Contributions

[#]These authors contributed equally. H.A.P., R.C.H., and M.P.M. conceived and designed the study. H.A.P. designed, performed, and analyzed most of the experiments and mass spectrometry assays. D.K.-A. and T.E.B. carried out *in vivo* work, supervised by T.K. and K.S.-P., respectively. L.P. and S.T.C. designed and synthesized compounds, supervised by R.C.H. A.M.J. advised on the experimental design and data interpretation. H.A.P. and M.P.M. wrote the manuscript with contribution from all other authors.

Notes

The authors declare the following competing financial interest(s): M.P.M., T.K, and K.S.-P. have submitted a patent application on the use of malonate esters to prevent I/R injury.

■ ACKNOWLEDGMENTS

We thank Angela Logan for helpful discussions on TPP mass spectrometry. Work in the MPM laboratory was supported by the Medical Research Council, UK (MC_U105663142), and by a Wellcome Trust Investigator award (110159/Z/15/Z). Work in the T.K. laboratory was supported by the British Heart Foundation (PG/15/84/31670) and Medical Research Council, UK (MR/P000320/1). Work in the R.C.H. laboratory was supported by a Wellcome Trust Investigator award (110158/Z/15/Z) and a PhD studentship for L.P. from the University of Glasgow. Work in the K.S.-P. laboratory was supported by the Medical Research Council UK.

■ ABBREVIATIONS

TPP, triphenylphosphonium; SDH, succinate dehydrogenase; RP-HPLC, reversed phase-high performance liquid chromatography; LC-MS/MS, liquid chromatography tandem mass spectrometry; RLM, rat liver mitochondria; RHM, rat heart mitochondria; ROS, reactive oxygen species; RET, reverse electron transfer; DIC, mitochondrial dicarboxylate carrier

■ REFERENCES

(1) Murphy, M. P.; Hartley, R. C. Mitochondria as a Therapeutic Target for Common Pathologies. *Nat. Rev. Drug Discovery* **2018**, *17* (12), 865−886.
(2) Nunnari, J.; Suomalainen, A. Mitochondria: In Sickness and in Health. *Cell* **2012**, *148* (6), 1145−1159.
(3) Gorman, G. S.; Chinnery, P. F.; DiMauro, S.; Hirano, M.; Koga, Y.; McFarland, R.; Suomalainen, A.; Thorburn, D. R.; Zeviani, M.; Turnbull, D. M. Mitochondrial Diseases. *Nat. Rev. Dis. Prim.* **2016**, *2* (1), 16080.
(4) Smith, R. A. J.; Hartley, R. C.; Cochemé, H. M.; Murphy, M. P. Mitochondrial Pharmacology. *Trends Pharmacol. Sci.* **2012**, *33*, 341−352.
(5) Jean, S. R.; Ahmed, M.; Lei, E. K.; Wisnovsky, S. P.; Kelley, S. O. Peptide-Mediated Delivery of Chemical Probes and Therapeutics to Mitochondria. *Acc. Chem. Res.* **2016**, *49* (9), 1893−1902.
(6) Smith, R. a. J.; Hartley, R. C.; Murphy, M. P. Mitochondria-Targeted Small Molecule Therapeutics and Probes. *Antioxid. Redox Signaling* **2011**, *15* (12), 3021.
(7) Dare, A. J.; Bolton, E. A.; Pettigrew, G. J.; Bradley, J. A.; Saeb-Parsy, K.; Murphy, M. P. Protection against Renal Ischemia−Reperfusion Injury in Vivo by the Mitochondria Targeted Antioxidant MitoQ. *Redox Biol.* **2015**, *5*, 163−168.
(8) Chouchani, E. T.; Methner, C.; Nadtochiy, S. M.; Logan, A.; Pell, V. R.; Ding, S.; James, A. M.; Cochemé, H. M.; Reinhold, J.; Lilley, K. S.; Partridge, L.; Fearnley, I. M.; Robinson, A. J.; Hartley, R. C.; Smith, R. A. J.; Krieg, T.; Brookes, P. S.; Murphy, M. P. Cardioprotection by S-Nitrosation of a Cysteine Switch on Mitochondrial Complex I. *Nat. Med.* **2013**, *19* (6), 753−759.
(9) Horton, K. L.; Stewart, K. M.; Fonseca, S. B.; Guo, Q.; Kelley, S. O. Mitochondria-Penetrating Peptides. *Chem. Biol.* **2008**, *15* (4), 375−382.
(10) Rokitskaya, T. I.; Sumbatyan, N. V.; Tashlitsky, V. N.; Korshunova, G. A.; Antonenko, Y. N.; Skulachev, V. P. Mitochondria-Targeted Penetrating Cations as Carriers of Hydrophobic Anions through Lipid Membranes. *Biochim. Biophys. Acta, Biomembr.* **2010**, *1798* (9), 1698−1706.
(11) Grinius, L. L.; Jasaitis, A. A.; Kadziauskas, Y. P.; Liberman, E. A.; Skulachev, V. P.; Topali, V. P.; Tsofina, L. M.; Vladimirova, M. A. Conversion of Biomembrane-Produced Energy into Electric Form. I. Submitochondrial Particles. *Biochim. Biophys. Acta, Bioenerg.* **1970**, *216* (1), 1−12.
(12) Ross, M. F.; Kelso, G. F.; Blaikie, F. H.; James, A. M.; Cochemé, H. M.; Filipovska, A.; Da Ros, T.; Hurd, T. R.; Smith, R. A. J.; Murphy, M. P. Lipophilic Triphenylphosphonium Cations as Tools in Mitochondrial Bioenergetics and Free Radical Biology. *Biochemistry* **2005**, *70* (2), 222−230.
(13) Shchepinova, M. M.; Cairns, A. G.; Prime, T. A.; Logan, A.; James, A. M.; Hall, A. R.; Vidoni, S.; Arndt, S.; Caldwell, S. T.; Prag, H. A.; Pell, V. R.; Krieg, T.; Mulvey, J. F.; Yadav, P.; Cobley, J. N.; Bright, T. P.; Senn, H. M.; Anderson, R. F.; Murphy, M. P.; Hartley, R. C. MitoNeoD: A Mitochondria-Targeted Superoxide Probe. *Cell Chem. Biol.* **2017**, *24* (10), 1285−1298.
(14) Rossman, M. J.; Santos-Parker, J. R.; Steward, C. A. C.; Bispham, N. Z.; Cuevas, L. M.; Rosenberg, H. L.; Woodward, K. A.; Chonchol, M.; Gioscia-Ryan, R. A.; Murphy, M. P.; Seals, D. R. Chronic Supplementation With a Mitochondrial Antioxidant (MitoQ) Improves Vascular Function in Healthy Older Adults. *Hypertension* **2018**, *71* (6), 1056−1063.
(15) Cheng, G.; Zielonka, J.; Hardy, M.; Ouari, O.; Chitambar, C. R.; Dwinell, M. B.; Kalyanaraman, B. Synergistic Inhibition of Tumor Cell Proliferation by Metformin and Mito-Metformin in the Presence of Iron Chelators. *Oncotarget* **2019**, *10* (37), 3518−3532.
(16) Booty, L. M.; Gawel, J. M.; Cvetko, F.; Caldwell, S. T.; Hall, A. R.; Mulvey, J. F.; James, A. M.; Hinchy, E. C.; Prime, T. A.; Arndt, S.; Beninca, C.; Bright, T. P.; Clatworthy, M. R.; Ferdinand, J. R.; Prag, H. A.; Logan, A.; Prudent, J.; Krieg, T.; Hartley, R. C.; Murphy, M. P. Selective Disruption of Mitochondrial Thiol Redox State in Cells and In Vivo. *Cell Chem. Biol.* **2019**, *26* (3), 449−461.
(17) Antonucci, S.; Mulvey, J. F.; Burger, N.; Di Sante, M.; Hall, A. R.; Hinchy, E. C.; Caldwell, S. T.; Gruszczyk, A. V.; Deshwal, S.; Hartley, R. C.; Kaludercic, N.; Murphy, M. P.; Di Lisa, F.; Krieg, T. Selective Mitochondrial Superoxide Generation in Vivo Is Cardioprotective through Hormesis. *Free Radical Biol. Med.* **2019**, *134*, 678−687.

(18) Methner, C.; Lukowski, R.; Grube, K.; Loga, F.; Smith, R. A. J.; Murphy, M. P.; Hofmann, F.; Krieg, T. Protection through Postconditioning or a Mitochondria-Targeted S-Nitrosothiol Is Unaffected by Cardiomyocyte-Selective Ablation of Protein Kinase G. *Basic Res. Cardiol.* **2013**, *108* (2), 337.
(19) Ruprecht, J. J.; Kunji, E. R. S. The SLC25 Mitochondrial Carrier Family: Structure and Mechanism. *Trends Biochem. Sci.* **2020**, *45* (3), 244−258.
(20) Ong, H. C.; Hu, Z.; Coimbra, J. T. S.; Ramos, M. J.; Kon, O. L.; Xing, B.; Yeow, E. K. L.; Fernandes, P. A.; García, F. Enabling Mitochondrial Uptake of Lipophilic Dications Using Methylated Triphenylphosphonium Moieties. *Inorg. Chem.* **2019**, *58* (13), 8293−8299.
(21) James, A. M.; Sharpley, M. S.; Manas, A.-R. B.; Frerman, F. E.; Hirst, J.; Smith, R. A. J.; Murphy, M. P. Interaction of the Mitochondria-Targeted Antioxidant MitoQ with Phospholipid Bilayers and Ubiquinone Oxidoreductases. *J. Biol. Chem.* **2007**, *282* (20), 14708−14718.
(22) Porteous, C. M.; Logan, A.; Evans, C.; Ledgerwood, E. C.; Menon, D. K.; Aigbirhio, F.; Smith, R. A. J.; Murphy, M. P. Rapid Uptake of Lipophilic Triphenylphosphonium Cations by Mitochondria in Vivo Following Intravenous Injection: Implications for Mitochondria-Specific Therapies and Probes. *Biochim. Biophys. Acta, Gen. Subj.* **2010**, *1800*, 1009.
(23) Cochemé, H. M.; Quin, C.; McQuaker, S. J.; Cabreiro, F.; Logan, A.; Prime, T. A.; Abakumova, I.; Patel, J. V.; Fearnley, I. M.; James, A. M.; Porteous, C. M.; Smith, R. A. J.; Saeed, S.; Carré, J. E.; Singer, M.; Gems, D.; Hartley, R. C.; Partridge, L.; Murphy, M. P. Measurement of H2O2 within Living Drosophila during Aging Using a Ratiometric Mass Spectrometry Probe Targeted to the Mitochondrial Matrix. *Cell Metab.* **2011**, *13* (3), 340−350.
(24) Kelso, G. F.; Porteous, C. M.; Coulter, C. V.; Hughes, G.; Porteous, W. K.; Ledgerwood, E. C.; Smith, R. A. J.; Murphy, M. P. Selective Targeting of a Redox-Active Ubiquinone to Mitochondria within Cells. *J. Biol. Chem.* **2001**, *276* (7), 4588−4596.
(25) Ripcke, J.; Zarse, K.; Ristow, M.; Birringer, M. Small-Molecule Targeting of the Mitochondrial Compartment with an Endogenously Cleaved Reversible Tag. *ChemBioChem* **2009**, *10* (10), 1689−1696.
(26) Prime, T. A.; Blaikie, F. H.; Evans, C.; Nadtochiy, S. M.; James, A. M.; Dahm, C. C.; Vitturi, D. A.; Patel, R. P.; Hiley, C. R.; Abakumova, I.; Requejo, R.; Chouchani, E. T.; Hurd, T. R.; Garvey, J. F.; Taylor, C. T.; Brookes, P. S.; Smith, R. A. J.; Murphy, M. P. A Mitochondria-Targeted S-Nitrosothiol Modulates Respiration, Nitrosates Thiols, and Protects against Ischemia-Reperfusion Injury. *Proc. Natl. Acad. Sci. U. S. A.* **2009**, *106* (26), 10764−10769.
(27) Finichiu, P. G.; James, A. M.; Larsen, L.; Smith, R. A. J.; Murphy, M. P. Mitochondrial Accumulation of a Lipophilic Cation Conjugated to an Ionisable Group Depends on Membrane Potential, PH Gradient and PK a: Implications for the Design of Mitochondrial Probes and Therapies. *J. Bioenerg. Biomembr.* **2013**, *45* (1−2), 165−173.
(28) Finichiu, P. G.; Larsen, D. S.; Evans, C.; Larsen, L.; Bright, T. P.; Robb, E. L.; Trnka, J.; Prime, T. A.; James, A. M.; Smith, R. A. J.; Murphy, M. P. A Mitochondria-Targeted Derivative of Ascorbate: MitoC. *Free Radical Biol. Med.* **2015**, *89*, 668−678.
(29) Kotlyar, A. B.; Vinogradov, A. D. Interaction of the Membrane-Bound Succinate Dehydrogenase with Substrate and Competitive Inhibitors. *Biochim. Biophys. Acta, Protein Struct. Mol. Enzymol.* **1984**, *784* (1), 24−34.
(30) Wang, H.; Huwaimel, B.; Verma, K.; Miller, J.; Germain, T. M.; Kinarivala, N.; Pappas, D.; Brookes, P. S.; Trippier, P. C. Synthesis and Antineoplastic Evaluation of Mitochondrial Complex II (Succinate Dehydrogenase) Inhibitors Derived from Atpenin A5. *ChemMedChem* **2017**, *12* (13), 1033−1044.
(31) Prag, H. A.; Pala, L.; Kula-Alwar, D.; Mulvey, J. F.; Luping, D.; Beach, T. E.; Booty, L. M.; Hall, A. R.; Logan, A.; Sauchanka, V.; Caldwell, S. T.; Robb, E. L.; James, A. M.; Xu, Z.; Saeb-Parsy, K.; Hartley, R. C.; Murphy, M. P.; Krieg, T. Ester Prodrugs of Malonate with Enhanced Intracellular Delivery Protect Against Cardiac Ischemia-Reperfusion Injury In Vivo. *Cardiovasc. Drugs Ther.* **2020**..
(32) Chouchani, E. T.; Pell, V. R.; Gaude, E.; Aksentijević, D.; Sundier, S. Y.; Robb, E. L.; Logan, A.; Nadtochiy, S. M.; Ord, E. N. J.; Smith, A. C.; Eyassu, F.; Shirley, R.; Hu, C.; Dare, A. J.; James, A. M.; Rogatti, S.; Hartley, R. C.; Eaton, S.; Costa, A. S. H.; Brookes, P. S.; Davidson, S. M.; Duchen, M. R.; Saeb-Parsy, K.; Shattock, M. J.; Robinson, A. J.; Work, L. M.; Frezza, C.; Krieg, T.; Murphy, M. P. Ischaemic Accumulation of Succinate Controls Reperfusion Injury through Mitochondrial ROS. *Nature* **2014**, *515* (7527), 431−435.
(33) Prag, H. A.; Gruszczyk, A. V.; Huang, M. M.; Beach, T. E.; Young, T.; Tronci, L.; Nikitopoulou, E.; Mulvey, J. F.; Ascione, R.; Hadjihambi, A.; Shattock, M. J.; Pellerin, L.; Saeb-Parsy, K.; Frezza, C.; James, A. M.; Krieg, T.; Murphy, M. P.; Aksentijević, D. Mechanism of Succinate Efflux upon Reperfusion of the Ischemic Heart. *Cardiovasc. Res.* **2020**, In press.
(34) Chappell, J. B.; Hansford, R. *Subcellular Components: Preparation and Fractionation*, 2nd ed.; Birnie, G., Ed.; Butterworth: London, UK, 1972.
(35) Sharpley, M. S.; Shannon, R. J.; Draghi, F.; Hirst, J. Interactions between Phospholipids and NADH:Ubiquinone Oxidoreductase (Complex I) from Bovine Mitochondria. *Biochemistry* **2006**, *45* (1), 241−248.
(36) Mills, E. L.; Ryan, D. G.; Prag, H. A.; Dikovskaya, D.; Menon, D.; Zaslona, Z.; Jedrychowski, M. P.; Costa, A. S. H.; Higgins, M.; Hams, E.; Szpyt, J.; Runtsch, M. C.; King, M. S.; McGouran, J. F.; Fischer, R.; Kessler, B. M.; McGettrick, A. F.; Hughes, M. M.; Carroll, R. G.; Booty, L. M.; Knatko, E. V.; Meakin, P. J.; Ashford, M. L. J.; Modis, L. K.; Brunori, G.; Sévin, D. C.; Fallon, P. G.; Caldwell, S. T.; Kunji, E. R. S.; Chouchani, E. T.; Frezza, C.; Dinkova-Kostova, A. T.; Hartley, R. C.; Murphy, M. P.; O'Neill, L. A. Itaconate Is an Anti-Inflammatory Metabolite That Activates Nrf2 via Alkylation of KEAP1. *Nature* **2018**, *556* (7699), 113−117.
(37) Robb, E. L.; Gawel, J. M.; Aksentijević, D.; Cochemé, H. M.; Stewart, T. S.; Shchepinova, M. M.; Qiang, H.; Prime, T. A.; Bright, T. P.; James, A. M.; Shattock, M. J.; Senn, H. M.; Hartley, R. C.; Murphy, M. P. Selective Superoxide Generation within Mitochondria by the Targeted Redox Cycler MitoParaquat. *Free Radical Biol. Med.* **2015**, *89*, 883−894.
(38) Kotapati, H. K.; Robinson, J. D.; Lawrence, D. R.; Fortner, K. R.; Stanford, C. W.; Powell, D. R.; Wardenga, R.; Bornscheuer, U. T.; Masterson, D. S. Diastereoselective Hydrolysis of Branched Malonate Diesters by Porcine Liver Esterase: Synthesis of 5-Benzyl-Substituted Cα-Methyl-β-Proline and Catalytic Evaluation. *Eur. J. Org. Chem.* **2017**, *2017* (20), 3009−3016.
(39) Breznik, M.; Kikelj, D. Pig Liver Esterase Catalyzed Hydrolysis of Dimethyl and Diethyl 2-Methyl-2-(o-Nitrophenoxy)Malonates. *Tetrahedron: Asymmetry* **1997**, *8* (3), 425−434.
(40) Zhou, Q.; Xiao, Q.; Zhang, Y.; Wang, X.; Xiao, Y.; Shi, D. Pig Liver Esterases PLE1 and PLE6: Heterologous Expression, Hydrolysis of Common Antibiotics and Pharmacological Consequences. *Sci. Rep.* **2019**, *9* (1), 15564.
(41) James, A. M.; Cochemé, H. M.; Smith, R. A. J.; Murphy, M. P. Interactions of Mitochondria-Targeted and Untargeted Ubiquinones with the Mitochondrial Respiratory Chain and Reactive Oxygen Species. *J. Biol. Chem.* **2005**, *280* (22), 21295−21312.
(42) Barton, P.; Laws, A. P.; Page, M. I. Structure−Activity Relationships in the Esterase-Catalysed Hydrolysis and Transesterification of Esters and Lactones. *J. Chem. Soc., Perkin Trans. 2* **1994**, *2* (9), 2021−2029.
(43) Blaha-Nelson, D.; Krüger, D. M.; Szeler, K.; Ben-David, M.; Kamerlin, S. C. L. Active Site Hydrophobicity and the Convergent Evolution of Paraoxonase Activity in Structurally Divergent Enzymes: The Case of Serum Paraoxonase 1. *J. Am. Chem. Soc.* **2017**, *139* (3), 1155−1167.
(44) Gerencser, A. A.; Chinopoulos, C.; Birket, M. J.; Jastroch, M.; Vitelli, C.; Nicholls, D. G.; Brand, M. D. Quantitative Measurement of Mitochondrial Membrane Potential in Cultured Cells: Calcium-

https://dx.doi.org/10.1021/acs.molpharmaceut.0c00533
Mol. Pharmaceutics 2020, 17, 3526−3540

Induced de- and Hyperpolarization of Neuronal Mitochondria. *J. Physiol.* **2012**, *590* (12), 2845−2871.
(45) Andersen, P. S.; Fuchs, M. Potential Energy Barriers to Ion Transport within Lipid Bilayers. Studies with Tetraphenylborate. *Biophys. J.* **1975**, *15* (8), 795−830.
(46) Morgan, E. W.; Yan, B. F.; Greenway, D.; Petersen, D. R.; Parkinson, A. Purification and Characterization of Two Rat-Liver Microsomal Carboxylesterases (Hydrolase A and B). *Arch. Biochem. Biophys.* **1994**, *315* (2), 495−512.
(47) Zoratti, M.; Favaron, M.; Pietrobon, D.; Petronilli, V. Nigericin-Induced Transient Changes in Rat-Liver Mitochondria. *Biochim. Biophys. Acta, Bioenerg.* **1984**, *767* (2), 231−239.
(48) Lin, T.-K.; Hughes, G.; Muratovska, A.; Blaikie, F. H.; Brookes, P. S.; Darley-Usmar, V.; Smith, R. A. J.; Murphy, M. P. Specific Modification of Mitochondrial Protein Thiols in Response to Oxidative Stress: A PROTEOMICS APPROACH. *J. Biol. Chem.* **2002**, *277* (19), 17048−17056.
(49) Smith, R. A. J.; Porteous, C. M.; Gane, A. M.; Murphy, M. P. Delivery of Bioactive Molecules to Mitochondria in Vivo. *Proc. Natl. Acad. Sci. U. S. A.* **2003**, *100* (9), 5407−5412.
(50) Brown, H. C.; McDaniel, D. H.; Hafliger, O. Dissociation Constants. In *Determination of Organic Structures by Physical Methods*; Braude, E. A., Nachod, F. C., Eds.; Elsevier, 1955; pp 567−662.
(51) Kanicky, J. R.; Shah, D. O. Effect of Premicellar Aggregation on the PKa of Fatty Acid Soap Solutions. *Langmuir* **2003**, *19* (6), 2034−2038.
(52) Hu, Z.; Sim, Y.; Kon, O. L.; Ng, W. H.; Ribeiro, A. J. M.; Ramos, M. J.; Fernandes, P. A.; Ganguly, R.; Xing, B.; García, F.; Yeow, E. K. L. Unique Triphenylphosphonium Derivatives for Enhanced Mitochondrial Uptake and Photodynamic Therapy. *Bioconjugate Chem.* **2017**, *28* (2), 590−599.
(53) Rokitskaya, T. I.; Luzhkov, V. B.; Korshunova, G. A.; Tashlitsky, V. N.; Antonenko, Y. N. Effect of Methyl and Halogen Substituents on the Transmembrane Movement of Lipophilic Ions. *Phys. Chem. Chem. Phys.* **2019**, *21* (42), 23355−23363.

https://dx.doi.org/10.1021/acs.molpharmaceut.0c00533
Mol. Pharmaceutics 2020, 17, 3526−3540